Published in final edited form as:

Clin Cancer Res. 2016 March 1; 22(5): 1185–1196. doi:10.1158/1078-0432.CCR-15-1015.

Preclinical efficacy of the MDM2 inhibitor RG7112 in *MDM2* amplified and *TP53* wild-type glioblastomas

Maite Verreault[1,2,3,4,11], **Charlotte Schmitt**[1,2,3,4], **Lauriane Goldwirt**[12], **Kristine Pelton**[8,9,10,14], **Samer Haidar**[8,9,10,14], **Camille Levasseur**[1,2,3,4], **Jeremy Guehennec**[1,2,3,4], **David Knoff**[8,9,10,14], **Marianne Labussiere**[1,2,3,4], **Yannick Marie**[1,2,3,4], **Azra H. Ligon**[9,10], **Karima Mokhtari**[1,2,3,4,5,6], **Khe Hoang-Xuan**[1,2,3,4,5,6], **Marc Sanson**[1,2,3,4,5,6], **Brian M Alexander**[13], **Patrick Y. Wen**[8,15], **Jean-Yves Delattre**[1,2,3,4,5,6], **Keith L. Ligon**[8,9,10,14,*], and **Ahmed Idbaih**[1,2,3,4,5,6,*]

[1]Inserm, U 1127, F-75013, Paris, France

[2]CNRS, UMR 7225, F-75013, Paris, France

[3]Sorbonne Universités, UPMC Univ Paris 06, UMR S 1127, F-75013, Paris, France

[4]Institut du Cerveau et de la Moëlle épinière, ICM, 47, Bd de l'Hôpital, F-75013, Paris, France

[5]AP-HP, Hôpital universitaire Pitié-Salpêtrière, Service de Neurologie 2-Mazarin, 47, Bd de l'Hopital, F-75013, Paris, France

[6]AP-HP, Hôpital de la Pitié-Salpêtrière, Service de Neuropathologie R Escourolle, 47, Bd de l'Hopital, F-75013, Paris, France

[7]OncoNeuroThèque biobank, Institut du Cerveau et de la Moëlle épinière, ICM, 47, Bd de l'Hopital, F-75013, Paris, France

[8]Department of Medical Oncology, Center for Molecular Oncologic Pathology, Dana-Farber Cancer Institute, 450 Brookline Ave, MA, Boston, Massachusetts, USA, 02115

[9]Department of Pathology, Brigham and Women's Hospital, 75, Francis Street, Boston, MA, USA, 02115

[10]Department of Pathology, Harvard Medical School, 25 Shattuck Street, Boston, MA, USA, 02115

[11]Institut du Cerveau et de la Moëlle épinière, Centre de neuroimagerie de recherche, CHU Pitié-Salpêtrière, 47, Bd de l'Hopital, 75013, Paris, France

[12]Laboratoire de Pharmacologie Biologique, Hôpital Saint-Louis, 1, avenue Claude-Vellefaux, 75010, Paris, France

Corresponding authors: Ahmed Idbaih, AP-HP, Hôpital universitaire Pitié-Salpêtrière, Service de Neurologie 2-Mazarin, 47, Bd de l'Hopital, F-75013, Paris, France. Tel: +33(0) 1 42 16 03 85. ahmed.idbaih@gmail.com. Keith L. Ligon, Department of Medical Oncology, Center for Molecular Oncologic Pathology, Dana-Farber Cancer Institute, 450 Brookline Ave, MA, Boston, Massachusetts, USA, 02115. Tel: (617) 632 2357. Keith_Ligon@dfci.harvard.edu.

*co-principal investigators

Conflict of Interest: PW is a member of a Roche advisory board. AI was funded by Roche to attend a medical meeting.

[13]Department of Radiation Oncology, Dana-Farber/Brigham and Women's Cancer Center, Harvard Medical School, 25 Shattuck Street, Boston, MA, USA, 02115

[14]Boston Children's Hospital, 300, Longwood avenue, Boston, MA 02115

[15]Department of Neurology, Brigham and Women's Hospital Boston, 75, Francis Street, Boston, MA, USA, 02115

Abstract

Rationale—p53 pathway alterations are key molecular events in glioblastoma (GBM). MDM2 inhibitors increase expression and stability of p53 and are presumed to be most efficacious in patients with *TP53* wild-type and *MDM2*-amplified cancers. However, this biomarker hypothesis has not been tested in patients or patient-derived models for GBM.

Methods—We performed a preclinical evaluation of RG7112 MDM2 inhibitor, across a panel of 36 patient-derived GBM cell lines (PDCLs), each genetically characterized according to their P53 pathway status. We then performed a pharmacokinetic (PK) profiling of RG7112 distribution in mice and evaluated the therapeutic activity of RG7112 in orthotopic and subcutaneous GBM models.

Results—*MDM2*-amplified PDCLs were 44 times more sensitive than *TP53* mutated lines that showed complete resistance at therapeutically attainable concentrations (avg. IC50 of 0.52 μM vs 21.9 μM). *MDM4* amplified PDCLs were highly sensitive but showed intermediate response (avg. IC50 of 1.2 μM), whereas response was heterogeneous in *TP53* wild-type PDCLs with normal MDM2/4 levels (avg. IC50 of 7.7 μM). In *MDM2*-amplified lines, RG7112 restored p53 activity inducing robust p21 expression and apoptosis. PK profiling of RG7112-treated PDCL intracranial xenografts demonstrated that the compound significantly crosses the blood-brain and the blood-tumor barriers. Most importantly, treatment of *MDM2*-amplified/*TP53* wild-type PDCL-derived model (subcutaneous and orthotopic) reduced tumor growth, was cytotoxic, and significantly increased survival.

Conclusion—These data strongly support development of MDM2 inhibitors for clinical testing in *MDM2*-amplified GBM patients. Moreover, significant efficacy in a subset of non-*MDM2* amplified models suggests that additional markers of response to MDM2 inhibitors must be identified.

Keywords

glioblastoma; MDM2 inhibitor; targeted therapy; *MDM2* amplification; *TP53* mutation

Introduction

Primary glioblastoma (GBM) is the most frequent and aggressive form of brain tumors in adults. Approximately 3 to 4 new cases per 100,000 people are diagnosed every year [1]. Despite intensive treatment including surgery, radiation therapy and cytotoxic chemotherapy, the prognosis of GBM patients remains poor, with a median survival of 12 to 24 months [2]. One promising strategy to improve therapy is to use small pharmacological molecules to target key molecular events driving gliomagenesis. In this context, a major effort has been

conducted by several teams worldwide including The Cancer Genome Atlas (TCGA) to identify pivotal molecular alterations in GBM with basic and clinical perspectives [3, 4].

The TCGA has demonstrated that the vast majority of GBM exhibits, through various genetic mechanisms, disruption of three major signaling pathways [4]: (i) tyrosine kinase receptor pathway, (ii) retinoblastoma pathway and (iii) p53 pathway. Deregulation of the core p53 pathway occurs in 43% of cases due to: (i) *TP53* gene mutation or homozygous deletion in 27.9% of cases, (ii) focal *MDM2* amplification in 8–9% of cases, and (iii) focal *MDM4* amplification in 7–9% of cases. However, it is hypothesized that restoration of *TP53* function may have significant therapeutic benefit in those patients without direct mutations in the *TP53* gene.

p53 is a transcription factor that responds to several forms of cellular stress [5]. The quantity of functional p53, together with a variety of factors that affect other signaling pathways, promotes events such as cell cycle arrest, DNA repair, cellular senescence or apoptosis to prevent tumor initiation or progression [5]. p53 activates a large number of targets, including the cell cycle regulator $p21^{WAF1}$ (p21) [6, 7]. One of the main modulators of functional p53 level is MDM2 proto-oncogene, E3 ubiquitin protein ligase (a.k.a. MDM2), which binds to p53 and induces its proteasome-mediated degradation [8]. Expression of the *MDM2* gene is p53-dependent, thus p53 controls the level of its own regulator MDM2 through a feedback loop [8]. MDM4 (also known as MDMX) is another regulator of p53 structurally related to MDM2, but acts differently on p53 by regulating its transcriptional activity rather than its protein level [9].

Several strategies to restore p53 tumor suppressive function, including MDM2 small molecule inhibitors, have been explored [10]. RG7112 (MDM2 Kd of 10.7 nm) has improved potency and pharmacological properties compared to Nutlin-3. It is the first MDM2 inhibitor to enter clinical trials, where its tolerability was confirmed in liposarcoma patients and was also recently reported to have clinical efficacy in leukemia [11, 12]. Tolerability was also assessed in a phase I trial in patients with advanced solid tumors and hematological neoplasms (NCT00559533), and results are pending. Based on their mechanisms of action, RG7112 and other agents in this class might be effective in patients with *MDM2* amplification and wild-type *TP53* tumor. However, studies to test this hypothesis have not been broadly performed in large numbers of genetically characterized patient derived cell lines or in the clinical trials performed to date. The study presented here aims to test the therapeutic activity of RG7112, a member of MDM2/Nutlin (cis-imidazoline) inhibitors [13], in GBM patient-derived cell lines (PDCL) and animal models of GBM carrying various alterations of the core p53 pathway (*MDM2* amplification, *MDM4* amplification, *TP53* mutation).

Material and methods

GBM cell lines and human GBM samples

U251, U87 and LN229 GBM cell lines were purchased from American Type Culture Collection (ATCC, Manassas, VA) and were cultured in DMEM supplemented with 10% fetal bovine serum (Gibco, Life Technologies, Saint-Aubin, France). SJSA-1 osteosarcoma

cell line (formerly OsA-CL) was purchased from ATCC and included in the present study as an *MDM2*-amplified positive control [14, 15]. Cells were cultured in DMEM/F12 + GlutaMax (Gibco, Life Technologies, Saint-Aubin, France) supplemented with 10% fetal bovine serum and were used within 6 months of culture after purchase of the lines. 3731, 4339, 7015 and 6215 patient-derived cell lines (PDCL) were established by the GlioTex team (Glioblastoma and Experimental Therapeutics) in the Institut du Cerveau et de la Moëlle épinière (ICM) laboratory and maintained in neurosphere growth conditions using DMEM/F12 (Gibco, Life Technologies, Saint-Aubin, France) culture medium supplemented with 1% penicillin/streptomycin, B27 (Gibco), EGF (20 ng/ml) and FGF (20 ng/ml) (Preprotech, Neuilly-sur-Seine, France). All PDCLs with a name starting with BT were established from tumors resected at Brigham and Women's Hospital and Boston Children's Hospital (Boston, USA) and were maintained in neurosphere growth conditions using NeuroCult™ NS-A Proliferation Kit (Stemcell Technologies, Vancouver, Canada) supplemented with 0.0002% heparin (Stemcell Technologies), EGF (20 ng/ml) and FGF (10 ng/ml) (Miltenyi, San Diego, USA). The identity of all cell lines established at the ICM or the Brigham and Women's Hospital and Boston Children's Hospital were confirmed by short tandem repeat assay and validated within 6 months of their use for the studies presented here. Cell line gene statuses are listed in S4. "*" indicates cell lines from the cohort #1 only, while the "**" indicates cell lines included in both cohort #1 and #2. "&" indicates cell lines that were included for the *in vivo* studies only. All other cell lines were part of the cohort #2.

Human GBM tissue samples were selected from OncoNeuroThèque (Institut du Cerveau et de la Moëlle épinière, Paris, France) tumor tissue bank. Tumor and annotations was collected with informed consent and with the relevant ethical board approval in accordance with the tenets of the Declaration of Helsinki. All cell lines were derived from patients with consent or waiver of consent by the appropriate institutional review board.

Proliferation assay

For drug sensitivity assays of the cohort #1 cell lines, 96-well plates were coated with 10 μg/mL laminin (#L2020, Sigma-Aldrich, Saint-Quentin Fallavier) at 37°C for 1 hour. Three thousand cells/well were then plated. RG7112 (gift from Roche TCRC, Nutley, USA) was resuspended as a 10 mM stock solution in DMSO and was added 24 h after plating. Seventy-two hours after drug addition, WST-1 reagent (Roche) was added according to the manufacturer's instructions. WST-1 salt is cleaved to a soluble formazan dye by a NAD(P)H-dependent reaction in viable cells. Plates were incubated for 3 h and read by spectrophotometry at 450 nm wavelength. For cohort #2 cell lines, cells were plated in 384-well format and a pin transfer robot (Epson) was used to transfer the compound solution (MedChemExpress) into each well, with 3 replicates per condition. Cell viability was measured after 72 hours of continuous drug exposure by CellTiter Glo luminescence assay (Promega). IC75, IC99, and IC100 (concentrations that induce a 75, 99, and 100% decrease in cell viability, respectively) were determined by least squares curve fitting using GraphPad® Prism 6.

In vivo efficacy orthotopic and heterotopic studies

All protocols involving work with live animals were reviewed and approved by the Ministère de l'Enseignement Supérieur et de la Recherche (Paris, France) or in accordance with Dana-Farber Cancer Institute animal facility regulations and policies under the protocol #09-016. For the orthotopic model, prior to inoculation, GBM cells were transduced with the luciferase gene (Gentaur, Paris, France). GBM cells were implanted (1.4×10^5 cells/2 μL) into the brain of Athymic Nude mice (7 weeks old females, 10 animals/group). A stereotaxic injection frame (David Kopf Instruments, Tujunga, USA) was used to inject cells into the right caudate nucleus-putamen (ML +0.15 mm; AP +0.1 cm; DV −0.25 mm). Animals were imaged weekly using the IVIS Spectrum (Perkin-Elmer, Waltham, USA) 10 minutes after injection of 2 mg luciferin (Promega, Charbonnieres, France). Animals were randomly assigned to treatment or vehicle arm when a signal of 1.10^6 photon/second was measured on their head.

For the heterotopic (subcutaneous) model, $2x10^6$ cells were resuspended in Hank's Buffered Salt Solution (Life Technologies), mixed with an equal volume of Matrigel (BD Biosciences, San Jose, USA) and injected into both flanks of eight-week-old NU/NU mice (Charles River, Wilmington, USA). Animals were randomly assigned to treatment or vehicle arm when tumors measured a volume of 200 mm^3. For both orthotopic and heterotopic models, animals were treated by gavage with 100 mg/kg of RG7112 formulation (100 mg/mL RG7112, 2% hydroxypropylcellulose, 0.1% Tween 80, 0.09% methylparaben and 0.01% propylparaben in water) or vehicle once per day, 5 days/week for 3 weeks. For the evaluation of GBM blood-brain barrier (BBB) integrity only, 1.2 mg of Hoechst 33342 (Sigma, Lyon, France) diluted in PBS was injected intravenously (iv) prior to termination. Mice were terminated by asphyxiation when they showed signs of tumor-associated illness or before reaching maximum subcutaneous tumor burden.

Pharmacokinetics studies

GBM cells were inoculated in the brain of Athymic Nude mice (Harlan, Gannat, France) as described below and animals were assigned to different pharmacokinetics time points when bioluminescence signal reached 1.10^8 photon/second. This threshold was selected to ensure that tumor volumes were as significant as possible without causing symptoms of pain or illness. The dose treatment solution of RG7112 (100 mg/mL RG7112) was prepared in a vehicle composed of 2% hydroxypropylcellulose, 0.1% Tween 80, 0.09% methylparaben and 0.01% propylparaben in water. Mice were sacrificed at 0, 1h, 2h, 4h, 8h, 24h and 48h post-gavage (3 mice per time point). Blood was collected via live cardiac puncture in polyethylene tubes using a heparinized syringe. Samples were immediately centrifuged at 5000 rpm for 15 min and plasma was removed and stored at −80°C until analysis. Whole brains were collected, rinsed with 0.9% sodium chloride. The right and left brain hemispheres were harvested separately and labeled as tumor hemisphere and counter hemisphere, respectively, and were frozen at −80°C. RG7112 levels in mice plasma, and brains were measured using validated liquid chromatography coupled with mass tandem spectrometry methods (TQS Quantum Ultra™, Thermo Scientific, Waltham, MA, USA).

Live cardiac puncture exsanguination was shown to remove most of the blood and intravascular drug from functional vessels, suggesting that perfusion prior to brain harvesting has limited impact on PK measurements [16]. Additionally, others [17] have suggested that no correction of apparent drug tissue concentrations for blood contamination was necessary for brain tissue, unless the brain-to-plasma ratio is below 0.1. The pharmacokinetic parameters Tmax (the time to reach peak concentration) and Cmax (the peak concentration) were thus calculated accordingly by non-compartmental analysis of mean concentration time data with WinNonlin (version 5.2, Pharsight, Mountain View, CA). It should be noted that this was a destructive sampling study design, hence, variability associated with the pharmacokinetic parameters other than $AUC_{0\text{-}t}$ could not be determined, and thus no statistical test was performed on these parameters.

Areas under the curve ($AUC_{0–t}$) for brain and plasma samples were calculated by using the trapezoidal rule. In this serial sampling design, only one measurement was available per animal, so the method developed by Bailer for destructive sampling was used to compare the AUCs ratios of brain/plasma concentrations between tumor and contralateral brain hemispheres [18].

The standard error of the mean concentrations y_i at time t_i, denoted sem_i, was estimated as the empirical standard deviation divided by r_i. Thus, the standard error of the AUC was estimated according to the equation:

$$SE^2\left[\overline{AUC}_{t_0}^{t_n}\right]=[0.5\times(t_1-t_0)\times sem_0]^2+\sum_{i=2}^{n}[0.5\times(t_i-t_{i-2})]^2+[0.5\times(t_n-t_{n-1})\times sem_n]^2$$

The test for equality of the mean AUCs between animal groups (CF1+/+ versus −/−) A and B was performed using the standard Wald statistic:

$$z_{obs}=\frac{\left[\overline{AUC}_A-\overline{AUC}_B\right]}{\sqrt{se^2(\overline{AUC}_A)+se^2(\overline{AUC}_B)}}$$

Under the null hypothesis that the mean AUCs are equal, this statistic follows a normal distribution. The null hypothesis was rejected if $|z|$ was greater than 1.96. A separate distribution study on subcutaneous tumor was also conducted. GBM cells were implanted subcutaneously in Athymic Nude mice (Harlan, Gannat, France and ICR SCID, Taconic). The RG7112 treatment solution (100 mg/mL) was prepared as described above and sacrifice was performed 48 h after gavage. Blood was collected via cardiac puncture in polyethylene tubes using a heparinized syringe. Samples were immediately centrifuged at 5000 rpm for 15 min and plasma was removed and stored at −80°C until analysis. The subcutaneous tumor was collected, rinsed with 0.9% sodium chloride and was frozen at −80°C. RG7112 levels in mouse plasma and tumor were measured using validated liquid chromatography coupled with mass tandem spectrometry methods (TQS Quantum Ultra™, Thermo Scientific, Waltham, MA, USA) and compared to plasma and brain hemispheres of GBM orthotopic-grafted mice sacrificed 48 h after drug administration.

Magnetic resonance imaging in mice

The MR images were acquired with a 11.7-T system (Bruker Biospec 117/16 USR horizontal bore, 750mT/m gradients, Paravision 5.1) and a CryoProbe™ (Bruker Biospin, Ettlingen, Germany). Anatomical T1-weighted images were acquired 3 weeks after bioluminescence signal reached 1.10^6 photon/second, before and after iv gadolinium injection with a 2D rapid acquisition relaxation enhanced (RARE) sequence; TR=500 ms; TE=10 ms; Matrix (Mtx)=128x128; field-of-view (FOV)=12.8x12.8 mm (resolution(res)=100x100 μm^2); slice thickness=400 μm; number of excitations (Nex)=1; RARE factor=1; scan time (Tacq)=1 min. Anatomical T2-weighted images were acquired prior to initiation of treatment (when bioluminescence signal reached 1.10^6 photon/second) and at the end of the 3 weeks treatment period with a 3D gradient-echo sequence with TR=16ms; TE=4.7ms; Mtx=192x192x128; FOV=19.2x19.2x12.8mm (resolution 100um isotropic voxel); Nex=3; Tacq=20min. Tumor volumes were estimated using the formula V= 5 4/3 π (a × b × c) where a, b, and c are the three radii [19].

Statistical analysis

All statistical data were collected using GraphPad Prism software (San Diego, CA). For protein and RNA level comparisons, p-values were calculated by comparing data measured from 3 independent experiments from each individual cell line with data from all the other cell lines. Parametric analysis was done using standard error of the mean, mean and n, in a multivariate one-way analysis (ANOVA) with Tukey's post-tests for multiple comparisons, and Student t-test for single comparisons. All data are shown as mean ± S.E.M. *p-value < 0.05; **p-value < 0.01; ***p-value < 0.001; ****p-value < 0.0001.

Overall survival was defined as the time between histological diagnosis and death or the last follow-up. Patients who were still alive at the last follow-up were considered as a censored event in the analysis. Survival curves were obtained according to the Kaplan-Meier method and differences between curves were assessed using the log-rank test. For survival comparisons in the orthotopic animal model, survival curves were obtained according to the Kaplan-Meier method and differences between curves were assessed using the log-rank test.

Results

MDM2 amplification does not impact prognosis in newly diagnosed GBM patients and is maintained at tumor recurrence

Data sets from the 2013 GBM TCGA database [4] (publically available on cBio portal; MSKCC) were extracted and analyzed. *TP53*, *MDM2* and *MDM4* were found to be genetically altered (*i.e.* gene copy number or sequence abnormalities) in 22%, 9% and 9%, respectively, of GBM from TCGA 2013 database. Graphs can be seen in supplementary data (S1). *MDM2*/*MDM4* alteration with concurrent *TP53* mutation was found to be a rare event detected in 1.37% of cases. Moreover, *MDM2* and *MDM4* amplifications were found to be mutually exclusive. Finally, as expected, MDM2 mRNA was found to be overexpressed in *MDM2*-amplified tumor (S1).

From the OncoNeuroThèque database, 696 newly diagnosed GBM with genomic profiling and clinical annotations were identified. Forty-three tumors out of 696 (6.2%) were *MDM2*-amplified. No statistical significance was detected between both groups for median overall survival (15.5 months in non-amplified vs 15.5 months in MDM2-amplified), age at diagnosis (57.4 versus 58.9 years in *MDM2*-amplified) and sex ratio (1.43 versus 1.39 in *MDM2*-amplified). Survival curve is provided in supplementary data (S2).

Among these patients, five *MDM2*-amplified GBM patients were re-operated at tumor recurrence once (4 patients) or twice (1 patient). Interestingly, *MDM2* amplification and *TP53* mutational status were maintained over time for all patients (S3).

PDCLs maintain genetic TP53 status heterogeneity observed in human GBM tumors

Thirty-six GBM cell lines including 32 PDCLs from two sets (cohort #1 and cohort #2, 4/32 PDCLs were used in both cohorts) and 4 commercially available cell lines were used in the present study. Data acquired from both cohorts were obtained from two independent laboratories. A summary of PDCL genetic status can be seen in supplementary data (S4). *MDM2* and *MDM4* high level amplifications were detected in 2/32 (BT484 and 3731) and 2/32 (BT112 and BT216) GBM PDCLs respectively, roughly equivalent with the incidence rate reported in patient samples in the TCGA dataset. *MDM2* and *MDM4* gain was seen in 3/32 and 2/32 PDCLs cell lines, respectively. Forteen out of the total cohort of 36 GBM lines carry *TP53* point mutations altering p53 functions. Most mutations were amino acid substitutions leading to a non-functional p53 protein. One cell line (BT320) exhibited *TP53* homozygous deletion. Although none of the *MDM2*-amplified cell lines carried *TP53* mutations, *MDM4*-amplified BT216 harbored *TP53* mutation.

MDM2, MDM4, and TP53 expression at mRNA level (S5) and at protein level were also quantified (S6) in 11 cell lines. The two *MDM2*-amplified cell lines (*i.e.* 3731 and BT484) overexpressed MDM2 mRNA and protein. Levels of MDM4 protein were statistically greater in *MDM4*-amplified line BT216 compared to non-amplified cell lines. Although a trend for increased MDM4 protein expression was observed in BT112 ($p=0.16$), the levels were not statistically different from the non-amplified lines. *TP53* homozygous mutant 4339 showed a significantly higher p53 protein expression, but the slight increase observed in *TP53* mutant U251 line was not found to be statistically different from the other wild-type lines. Accumulation of p53 protein was not detected in *TP53* mutant BT216.

RG7112 exhibits greatest efficacy in MDM2-amplified GBM cell lines

The impact of RG7112 on cell viability was first assessed in 11 GBM cell lines (cohort #1, AI). The IC50s after exposure for 72 h is shown in Figure 1, panel B, and were derived from dose-response curves (Figure 1, panel A). The IC50s of both cell lines carrying *MDM2* gene amplification and wild-type *TP53* (3731 and BT484) are 37 times lower than that of *TP53* mutated and/or *MDM2/4* non-amplified cell lines. *MDM4*-amplified BT112 and *MDM2*-gained DKMG lines were 7 and 3.5 times more sensitive than *TP53* mutant and/or *MDM2/4* non-amplified cell lines, respectively. The IC50s of *TP53* homozygous mutant cell lines (4339, U251 and BT216) were not different from those of *TP53* wild-type/*MDM2*/*4* non-amplified lines (7015, 6215, LN229 and U87).

Validation experiments were conducted in an independent lab (cohort #2; KL). *MDM2*-amplified cell lines (3731 and BT484) were found to be highly sensitive to the inhibitor (average IC50 of 0.52 μM), whereas all cell lines carrying a *TP53* genetic alteration showed marked resistance to the inhibitor, with an average IC50 of 21.9 μM (42-fold increase). The *MDM4*-amplified line BT112 together with all lines carrying gains in *MDM2* or *MDM4* showed intermediate sensitivity (average IC50 of 1.5 μM). Overall, *MDM2/4*-amplified/gained lines and *TP53* wild-type were 18-fold and 2.8-fold, respectively, more sensitive than the *TP53* mutated/deleted cell lines (Figure 1, Panel C).

RG7112 restores p53 signaling pathway in MDM2-amplified cell lines in vitro

Protein levels of p53 and its downstream effector p21 were assessed by immunofluorescence in 3731$^{MDM2_Amp/TP53_Wt}$, 4339$^{MDM2/4_NL/TP53_Mt}$ and 7015$^{MDM2/4_NL/TP53_Wt}$ (Figure 2, Panel A and B). A 24 h exposure to IC100 restored p53 and p21 expression in *MDM2*-amplified 3731. This time point was selected because signs of cell death started to occur only 20–25 h after addition of RG7112, an observation that is consistent with a previously published report [20]. In 4339$^{MDM2/4_NL/TP53_Mt}$, p53 protein level was also increased by the treatment, whereas p21 level was not significantly affected. Finally, in 7015$^{MDM2/4_NL/TP53_Wt}$, p53 level remained unchanged but p21 protein level was found to be decreased.

Protein levels of p53 and p21 as well as MDM2 were also assessed by Western Blot in 3731$^{MDM2_Amp/TP53_wt}$ following a 24 h exposure to 0.5 μM, 1.5 μM and 4 μM RG7112 which were calculated to be the IC75, IC99 and IC100, respectively, when cells are exposed over to the drug over 72 h (Figure 2, Panel C). p21, p53 and MDM2 protein levels were significantly increased by RG7112.

RG7112 crosses the blood-brain barrier and the blood-tumor barrier

A key question related to the imidazole class of MDM2 inhibitors has been to what extent their relatively larger size might limit their penetration across the blood-brain barrier (BBB). First, in order to assess the permeability of the BBB in GBM tumor generated by 3731$^{MDM2_Amp/TP53_Wt}$ PDCL, this line was engrafted in the putamen of mice. T1-weighted MRI (Figure 3, Panel A–B) showed marked gadolinium contrast enhancement 130 days after inoculation, consistent with a partial disruption of the BBB in this model. Further assessment of BBB disruption was also performed with Hoechst 33342 injected intravenously in animals prior to sacrifice. Whereas Hoechst staining was not detected in normal brain tissue, staining was found in tumor tissue, mainly in the center of tumors and in the vicinity of tumor blood vessels (Figure 3C–D). Taken together, these data suggest a partial disruption of the BBB in this *MDM2*-amplified GBM model compared to the normal brain.

Pharmacokinetic profiling of RG7112 in the plasma, tumor cells-grafted hemisphere and contralateral hemisphere was conducted in 3731$^{MDM2_Amp/TP53_Wt}$ GBM-bearing mice (treatment started on an average of 80 days after inoculation; Figure 3, Panel E). Tmax were 2 to 8 h, 2 h and 8 h in the plasma, grafted and contralateral hemispheres, respectively. Cmax were 17178 ng/mL, 3328 ng/g (equivalent to 4.8 μM) and 2025 ng/g (equivalent to 2.9 μM)

in plasma, grafted and contralateral hemispheres, respectively. All of these Cmax were well above the mean IC50 calculated from *in vitro* studies for the 3731$^{MDM2_Amp/TP53_Wt}$ cell line (0.5 μM). Finally, brain tissue-to-plasma AUCs ratio was significantly greater (1.9-fold) in tumor-grafted hemispheres compared to contralateral non-tumor hemispheres (0,198 vs 0,106 $ng.h.g^{-1}/ng.h.mL^{-1}$ in grafted and contralateral hemispheres, respectively, z=−4.07; Figure, panel F). Interestingly, RG7112 distribution was 22-fold higher in subcutaneous tumor than in tumor-grafted hemispheres with a subcutaneous tumor-to-plasma ratio reaching 6.08 48 h after drug administration (Figure 3, panel G). This observation suggests that the blood-brain barrier is only partially disrupted in the grafted-hemisphere.

RG7112 reduces tumor growth rate and increases survival in heterotopic and orthotopic animal models bearing MDM2-amplified GBM

The *in vivo* efficacy of RG7112 was first assessed in subcutaneous GBM (3731$^{MDM2_Amp/TP53_Wt}$, BT139$^{MDM2/4_NL/TP53_Wt}$, BT182$^{MDM2/4_NL/TP53_Wt}$ and 4339$^{MDM2/4_NL/TP53_Mt}$) and osteosarcoma (SJSA$^{MDM2_Amp/TP53_Wt}$) models (Figure 4). Interestingly, similarly to what was observed with the SJSA$^{MDM2_Amp/TP53_Wt}$ model, a complete tumor growth suppression, and even a 80% regression, was achieved in the 3731$^{MDM2_Amp/TP53_Wt}$ model during the 21 day treatment period (p-value=0.003), but tumors rapidly re-emerged within days of withdrawing treatment. A slight but not statistically different reduction in growth rate was also observed in the *TP53* wild-type models (BT139 and BT182), however the treatment did not induce tumor regression. Finally, RG7112 appeared to be inactive in a *TP53* mutant model (4339). Taken together, these observations correlate with the data observed *in vitro*.

The efficacy of RG7112 (100 mg/kg) was then assessed in the *MDM2*-amplified 3731 orthotopic GBM *in vivo* model. RG7112 decreased tumor progression rate as shown by bioluminescence imaging curves (Figures 5, Panels A–C). This decrease of tumor growth was validated on T2-weighted MRI anatomical images (Figure 5, Panel D). The tumor volume decreased from 4.91 mm^3 prior to RG7112 treatment to 4.28 mm^3 at the end of treatment (13% decrease). In contrast, tumor volume increased from 5.97 to 84.84 mm^3 in vehicle-treated tumors, representing a 14.2-fold volume increase in these animals. Finally, RG7112 prolonged survival of tumor-bearing mice treated with RG7112 *versus* vehicle-treated mice (p=0.0003; Figure 5, Panel B).

Pharmodynamic studies

A pharmacodynamic study was also conducted in subcutaneous GBM models, where tumor-bearing animals were treated for 48 h with RG7112 and subsequently analyzed for effect on pathway dynamics (Figure 6). The expression of Ki67, a proliferation marker, was reduced by the treatment in all models. Cleaved caspase-3 (CC3), an apoptosis marker, was increased by the treatment in all models, indicating a strong cytotoxic effect (Figure 6 A–D, F). Finally, protein expression of MDM2, p53 and p21 was also increased by the treatment in all models compared to untreated (vehicle) animals as shown by IHC (Figure 6 A–D, F) and western blot (Figure 6, panel E).

p53 and p21 protein expression was also assessed in the orthotopic model at the end of the 21-days treatment period (Figure 6, panel G). However, none of these markers were statistically different in treated animals compared to untreated ones.

Orthotopic tumors at recurrence after RG7112 treatment were characterized as well. Treated and untreated animals were sacrificed when they showed signs of illness, which occurred at 19–31 days and 3–19 days after the end of the treatment period, respectively. Figure 6, Panel H shows that p53 protein level only (and not p21) was increased in recurrent tumors of treated animals compared to untreated tumors. The *TP53* gene was sequenced by Sanger sequencing in these tumors, but no mutation was detected. *MDM2* amplification level was quantified by Taqman assay and the amplification level was unchanged between treated and untreated animals.

Discussion

Translational research is now largely influenced by the approach of molecular personalized therapy. Indeed, molecular targeting has dramatically changed the prognosis of multiple aggressive cancers (*e.g.* gastrointestinal stromal tumor or metastatic melanoma) exhibiting a specific actionable molecular alteration [21, 22].

In this study, we have evaluated the activity of one of the most promising MDM2 inhibitor, RG7112, in a panel of GBM PDCL carrying different molecular alterations of p53 core pathway that are frequently found in human GBM. The experiments were conducted on a large set of GBM PDCL in two independent laboratories to validate the findings.

The GBM PDCL used in the present study carried alterations of p53 core pathway in proportions that were similar to what is found in human GBM. Indeed, *TP53* mutation/deletion, *MDM2*/4 amplifications or gains, which are generally mutually exclusive, were observed in 41.7%, 13.9% and 13.9% of our cell lines, respectively. *MDM2*/*4* amplifications were associated with increased protein expression. *TP53* mutation was associated with accumulation of p53 protein in two of the three *TP53* mutated cell lines assessed. The absence of detected p53 protein in BT216 can be explained by the fact that deletion mutations resulting in truncated protein do not lead to detectable protein accumulation [23, 24].

In vitro studies revealed that PDCL$^{MDM2_\mathrm{Amp}}$ were approximately 40 times more sensitive to RG7112 than the other lines. A 24 h exposure to RG7112 restored p53 and p21 protein expression in PDCL$^{MDM2_\mathrm{Amp}}$. In addition, MDM2 expression was also increased, probably due to an increased transcription of the gene induced by p53 [8]. It can thus be presumed that cell death occurred through a p53-driven mechanism in these cells. While PDCL$^{TP53_\mathrm{Wt}}$ showed intermediate and variable sensitivity, PDCL$^{TP53_\mathrm{Mt}}$ or PDCL$^{TP53_\mathrm{Deleted}}$ were resistant to RG7112. The IC50s reported in this study are consistent with previous reports showing that *MDM2* amplified cancer cell lines (*e.g.* liposarcoma and osteosarcoma lines) are more sensitive to RG7112 or Nutlin-3 [25–28].

Interestingly, PDCL$^{MDM4_\mathrm{Amp}/TP53_\mathrm{Wt}}$ and PDCL$^{MDM4_\mathrm{Gain}/TP53_\mathrm{Wt}}$ also showed considerable sensitivity to the compound, which was unexpected, as Nutlin compounds have

a 100-fold greater affinity for MDM2 over MDM4 [13]. *MDM4* amplification was even shown to reduce sensitivity of cells to Nutlin-3 [29–31]. However, as suggested [13], p53 induced up-regulation of MDM2 might promote MDM4 degradation in some cell lines, which, in turn, would activate apoptosis cascade. These observations will need to be confirmed using additional cell lines harboring these alterations.

Overall, our *in vitro* data suggested that RG7112 is active in GBM cells. We thus proceeded with *in vivo* pharmacokinetics and efficacy studies. We showed that the compound absorption from oral administration was fairly rapid, as the plasma C_{max} was achieved within 2 h. Plasma $AUC_{0–48hrs}$ (420,253 ng·h·mL^{-1}) following a single dose of 100 mg/kg RG7112 was consistent with a previous study that reported an AUC of 250,000 ng·h·mL^{-1} preclinically in mice with a dose of 50 mg/kg [32]. Pharmacokinetic study conducted in contralateral hemispheres of tumor-bearing mice showed that RG7112 crosses the normal blood-brain barrier with a brain-to-plasma AUC ratio of 0.106, which is consistent with preliminary pharmacokinetics data obtained in healthy mice in our laboratory (data not shown).

A lack of data on the degree to which existing MDM2 inhibitors might penetrate the BBB or blood tumor barrier and have efficacy has limited studies in GBM. After demonstrating that the BBB is partially disrupted in our GBM mouse models using Hoechst dye [33, 34] and brain MRI with gadolinium infusion, we showed that RG7112 crosses pathologic blood-brain and blood-tumor barriers with a brain-to-plasma AUC ratio of 0.198. Interestingly, the T_{max} in the tumor hemisphere was achieved within 2 h compared to 8 h in the contralateral hemisphere, and the AUC in the grafted hemisphere was almost twice the $AUC_{contralat.}$, suggesting that RG7112 penetrates more easily the tumor tissue. However, the much higher concentration in the subcutaneous tumor suggests that the BBB is only partially disrupted in the brain tumor. It is important to note, that, because of the nature of GBM tumor vasculature, which was shown to comprise between 30–50% of poorly perfused vessels [35], we cannot exclude the possibility of a contribution from intravascular drug and blood in our brain tissue AUCs calculations.

Most importantly, we demonstrated that RG7112 is active in our *in vivo MDM2*-amplified GBM models. The 3 weeks treatment led to a 50% increase in median survival of orthotopic tumor-bearing animals. Whereas a stabilized disease was observed in the orthotopic 3731^{MDM2_Amp} model, a complete inhibition of tumor growth was observed in the subcutaneous model, suggesting a greater efficacy of RG7112 in the subcutaneous model compared to the orthotopic model. This increased efficacy could be explained by the much greater drug quantity measured in subcutaneous tumors compared to orthotopic tumors. In the clinic, RG7112 treatment of *MDM2*-amplified liposarcoma patients resulted in a stable disease (14 out of 20 patients) or a partial response (1 out of 20 patients) [11]. The data reported here in the orthotopic model is coherent with this observation, as tumor growth was inhibited by the treatment, but seemed to be reinitiated when the treatment was halted. In this same clinical study, increased p53, p21 and MDM2 protein expression and decreased Ki67 expression were observed in the tumor after the first 6–10 days cycle of daily RG7112 administration [11]. In our study, increased expression of p53, p21, MDM2 and decreased

expression of Ki67 were also measured in subcutaneous treated tumors 48 h after RG7112 dosing.

In both orthotopic and subcutaneous models, it appears that inhibition of MDM2 prevented tumor growth. However, when the treatment was stopped, tumor growth was reinitiated, suggesting that RG7112 is efficacious but of limited duration. Moreover, the expression of MDM2, p53, p21, Ki67 and CC3 markers were assessed in orthotopic tumors that were treated for 3 weeks and, although trends were observed, no statistically significant changes were observed. This suggests that tumor concentration of RG7112 was not high enough at that point to induce detectable changes in the expression of these markers, or that resistance mechanisms had been activated. Panel 6H proposes a possible mechanism of resistance to MDM2 inhibition. An increase in p53 expression (but not p21 nor MDM2) was observed in tumors at relapse, potentially associated with the emergence of *TP53* mutant tumor cell subpopulations, as it was reported previously (reviewed in [36]). However, *TP53* sequencing of these tumors did not reveal any mutations, possibly because these cells were not abundant enough in the tumor tissue. *In vitro* studies including a comprehensive assessment of molecular characteristics of cells exposed to RG7112 for an extended period of time could help identify resistance mechanisms and propose combination therapies to improve RG7112 therapeutic efficacy. For example, temozolomide was previously shown to act synergistically with RG7112 [37]. Other MDM2 inhibitors were shown to enhance sensitivity to radiation in human xenografts [38, 39]. In addition to confirming our data using other *in vivo* models, future studies will include testing of such combinations, as well as the evaluation of more potent MDM2 inhibitors including those in clinical trials (RG7388) [40, 41].

Some severe adverse effects were reported in a phase I trial of RG7112 in patients: neutropenia in six out of 20 patients and thrombocytopenia in three out of 20 patients [11]. We thus believe that the present study strongly supports research towards the development of MDM2 inhibitors as a class for clinical testing in GBM patients, whether it be with RG7112 or, perhaps, more potent MDM2 inhibitors that are associated with less severe adverse effects. Although additional markers predictive of response to the inhibitor in *TP53* wild-type GBM should be identified and therapeutic benefit of RG7112 for *MDM4* amplified/gained GBM patients remains to be further investigated, data shown here and observations made in the context of other clinical trials for RG7112 [42] suggest that, in future clinical trials, patients with *MDM2*-amplified/gained GBM should be included. Our analysis on the evolution of *MDM2* amplification and *TP53* wild type statuses over time showed that these statuses remain unchanged during the course of the disease. This observation facilitates the design of a RG7112 clinical trial in GBM, as the burden of reassessing *MDM2* and *TP53* statuses at recurrence could be avoided. However, others have proposed that a larger epigenetic and expression profiling of a subset of *TP53* target genes should be used to predict treatment response instead of the traditional *MDM2* amplified/*TP53* wild-type profile [43]. Interestingly, in our study, we observed that a subset of PDCLs that carried a *CDKN2A* homozygous deletion together with wild-type *TP53* were more sensitive than *CDKN2A* wild-type lines. Therefore, significant efficacy in a subset of non-*MDM2* amplified models suggests that RG7112 and other MDM2 inhibitors may not be solely efficacious in *MDM2*-amplified tumors, and additional biomarkers predictive of response to the inhibitor in other genotypes need to be identified. The design of a trial for testing MDM2

inhibitors in GBM could thus possibly include a smaller cohort where a more thorough profiling, including *TP53* pathway up- and downstream genes, is performed.

In all cases, our analysis of the impact of *MDM2* status on prognosis supports other analysis [44] and shows that the fate of *MDM2*-amplified GBM patients is as unfortunate as that of all other GBM patients. The considerable sensitivity of *MDM2*-amplified GBM to RG7112 thus suggests a potential clinical benefit of MDM2 inhibitors for those 8–9% of GBM patients whose tumor carries this genomic alteration.

Supplementary Material

Refer to Web version on PubMed Central for supplementary material.

Acknowledgments

Funding information: This work is part of the GlioTex (i.e., Glioblastoma and Experimental Therapeutics) project funded by La Fondation ARC pour la Recherche sur le Cancer and supported by L'Institut Universitaire de Cancérologie (IUC). Additional support for this work was received from the DFCI Brain Tumor Therapeutics Accelerator Program (to P.Y. Wen) and the National Cancer Institute of the National Institutes of Health under award numbers P50CA165962 (to P.Y. Wen and K.L. Ligon), R01CA170592 (to P.Y. Wen and K.L. Ligon), R01 CA188228 (to K.L. Ligon and R. Beroukhim) and P01CA142536 (to K.L. Ligon).

Animal studies were performed with the technical support of staff of the Pitié-Salpêtrière Functional Experimentation Center and the Animal Resource Facility at Dana-Farber Cancer Institute in Boston. We thank the Harvard ICCB-Longwood Screening Facility for assistance with screening. MRI data were acquired by the Center for Neuroimaging Research (CENIR) who has received funding from the program "Investissements d'avenir" ANR-10-IAIHU-06, from the Ile-de-France Region (DIM Cerveau et Pensée), and from IPRIAC (Institution de Prévoyance d'Inaptitude à la Conduite).

References

1. Ostrom QT, Bauchet L, Davis FG, Deltour I, Fisher JL, Langer CE, et al. The epidemiology of glioma in adults: a "state of the science" review. Neuro Oncol. 2014; 16(7):896–913. [PubMed: 24842956]
2. Stupp R, Hegi ME, Mason WP, van den Bent MJ, Taphoorn MJ, Janzer RC, et al. Effects of radiotherapy with concomitant and adjuvant temozolomide versus radiotherapy alone on survival in glioblastoma in a randomised phase III study: 5-year analysis of the EORTC-NCIC trial. Lancet Oncol. 2009; 10(5):459–66. [PubMed: 19269895]
3. TCGAP. Comprehensive genomic characterization defines human glioblastoma genes and core pathways. Nature. 2008; 455(7216):1061–8. [PubMed: 18772890]
4. Brennan CW, Verhaak RG, McKenna A, Campos B, Noushmehr H, Salama SR, et al. The somatic genomic landscape of glioblastoma. Cell. 2013; 155(2):462–77. [PubMed: 24120142]
5. Fridman JS, Lowe SW. Control of apoptosis by p53. Oncogene. 2003; 22(56):9030–40. [PubMed: 14663481]
6. Mirzayans R, Andrais B, Scott A, Murray D. New insights into p53 signaling and cancer cell response to DNA damage: implications for cancer therapy. J Biomed Biotechnol. 2012; 2012:170325. [PubMed: 22911014]
7. Roos WP, Kaina B. DNA damage-induced cell death by apoptosis. Trends Mol Med. 2006; 12(9): 440–50. [PubMed: 16899408]
8. Meek DW, Hupp TR. The regulation of MDM2 by multisite phosphorylation--opportunities for molecular-based intervention to target tumours? Semin Cancer Biol. 20(1):19–28. [PubMed: 19897041]
9. Toledo F, Wahl GM. MDM2 and MDM4: p53 regulators as targets in anticancer therapy. Int J Biochem Cell Biol. 2007; 39(7–8):1476–82. [PubMed: 17499002]

10. Stegh AH. Targeting the p53 signaling pathway in cancer therapy - the promises, challenges and perils. Expert Opin Ther Targets. 16(1):67–83. [PubMed: 22239435]
11. Ray-Coquard I, Blay JY, Italiano A, Le Cesne A, Penel N, Zhi J, et al. Effect of the MDM2 antagonist RG7112 on the P53 pathway in patients with MDM2-amplified, well-differentiated or dedifferentiated liposarcoma: an exploratory proof-of-mechanism study. Lancet Oncol. 2012; 13(11):1133–40. [PubMed: 23084521]
12. Andreeff, M.; Kelly, KR.; Yee, K.; Assouline, S.; Strair, R.; Popplewell, L., et al. Results of the Phase 1 Trial of RG7112, a Small-Molecule MDM2 Antagonist, in Acute Leukemia. 54th ASH Annual Meeting and Exposition Abstract book; 2012; p. Abstract 675
13. Kumar WZBA. Targeting the MDM2-p53 Protein-Protein Interaction for New Cancer Therapeutics.
14. Oliner JD, Kinzler KW, Meltzer PS, George DL, Vogelstein B. Amplification of a gene encoding a p53-associated protein in human sarcomas. Nature. 1992; 358(6381):80–3. [PubMed: 1614537]
15. Florenes VA, Maelandsmo GM, Forus A, Andreassen A, Myklebost O, Fodstad O. MDM2 gene amplification and transcript levels in human sarcomas: relationship to TP53 gene status. J Natl Cancer Inst. 1994; 86(17):1297–302. [PubMed: 8064888]
16. Friden M, Ljungqvist H, Middleton B, Bredberg U, Hammarlund-Udenaes M. Improved measurement of drug exposure in the brain using drug-specific correction for residual blood. J Cereb Blood Flow Metab. 2010; 30(1):150–61. [PubMed: 19756019]
17. Giudicelli C, Dricot E, Moati F, Strolin-Benedetti M, Giudicelli JF. Is it important to correct apparent drug tissue concentrations for blood contamination in the dog? Fundam Clin Pharmacol. 2004; 18(3):281–6. [PubMed: 15147279]
18. Bailer AJ. Testing for the equality of area under the curves when using destructive measurement techniques. J Pharmacokinet Biopharm. 1988; 16(3):303–9. [PubMed: 3221328]
19. Sorensen AG, Patel S, Harmath C, Bridges S, Synnott J, Sievers A, et al. Comparison of diameter and perimeter methods for tumor volume calculation. J Clin Oncol. 2001; 19(2):551–7. [PubMed: 11208850]
20. Tovar C, Graves B, Packman K, Filipovic Z, Higgins B, Xia M, et al. MDM2 small-molecule antagonist RG7112 activates p53 signaling and regresses human tumors in preclinical cancer models. Cancer Res. 2013; 73(8):2587–97. [PubMed: 23400593]
21. Chapman PB, Hauschild A, Robert C, Haanen JB, Ascierto P, Larkin J, et al. Improved survival with vemurafenib in melanoma with BRAF V600E mutation. N Engl J Med. 2011; 364(26):2507–16. [PubMed: 21639808]
22. Demetri GD, von Mehren M, Blanke CD, Van den Abbeele AD, Eisenberg B, Roberts PJ, et al. Efficacy and safety of imatinib mesylate in advanced gastrointestinal stromal tumors. N Engl J Med. 2002; 347(7):472–80. [PubMed: 12181401]
23. Anker L, Ohgaki H, Ludeke BI, Herrmann HD, Kleihues P, Westphal M. p53 protein accumulation and gene mutations in human glioma cell lines. Int J Cancer. 1993; 55(6):982–7. [PubMed: 8253536]
24. Rasheed BK, McLendon RE, Herndon JE, Friedman HS, Friedman AH, Bigner DD, et al. Alterations of the TP53 gene in human gliomas. Cancer Res. 1994; 54(5):1324–30. [PubMed: 8118823]
25. Arva NC, Talbott KE, Okoro DR, Brekman A, Qiu WG, Bargonetti J. Disruption of the p53-Mdm2 complex by Nutlin-3 reveals different cancer cell phenotypes. Ethn Dis. 2008; 18(2 Suppl 2):S2–1. [PubMed: 18646312]
26. Muller CR, Paulsen EB, Noordhuis P, Pedeutour F, Saeter G, Myklebost O. Potential for treatment of liposarcomas with the MDM2 antagonist Nutlin-3A. Int J Cancer. 2007; 121(1):199–205. [PubMed: 17354236]
27. Wang B, Fang L, Zhao H, Xiang T, Wang D. MDM2 inhibitor Nutlin-3a suppresses proliferation and promotes apoptosis in osteosarcoma cells. Acta Biochim Biophys Sin (Shanghai). 44(8):685–91. [PubMed: 22843172]
28. Tovar C, Graves B, Packman K, Filipovic Z, Higgins B, Xia M, et al. MDM2 small-molecule antagonist RG7112 activates p53 signaling and regresses human tumors in preclinical cancer models. Cancer Res. 73(8):2587–97. [PubMed: 23400593]

29. Hu B, Gilkes DM, Farooqi B, Sebti SM, Chen J. MDMX overexpression prevents p53 activation by the MDM2 inhibitor Nutlin. J Biol Chem. 2006; 281(44):33030–5. [PubMed: 16905541]
30. Patton JT, Mayo LD, Singhi AD, Gudkov AV, Stark GR, Jackson MW. Levels of HdmX expression dictate the sensitivity of normal and transformed cells to Nutlin-3. Cancer Res. 2006; 66(6):3169–76. [PubMed: 16540668]
31. Wade M, Wong ET, Tang M, Stommel JM, Wahl GM. Hdmx modulates the outcome of p53 activation in human tumor cells. J Biol Chem. 2006; 281(44):33036–44. [PubMed: 16905769]
32. Vu B, Wovkulich P, Pizzolato G, Lovey A, Ding Q, Jiang N, et al. Discovery of RG7112: A Small-Molecule MDM2 Inhibitor in Clinical Development. ACS Med Chem Lett. 2013; 4(5):466–9. [PubMed: 24900694]
33. Bernsen HJ, Rijken PF, Hagemeier NE, van der Kogel AJ. A quantitative analysis of vascularization and perfusion of human glioma xenografts at different implantation sites. Microvasc Res. 1999; 57(3):244–57. [PubMed: 10329251]
34. Verreault M, Strutt D, Masin D, Anantha M, Yung A, Kozlowski P, et al. Vascular normalization in orthotopic glioblastoma following intravenous treatment with lipid-based nanoparticulate formulations of irinotecan (Irinophore C), doxorubicin (Caelyx(R)) or vincristine. BMC Cancer. 2011; 11(124)
35. Vajkoczy P, Menger MD. Vascular microenvironment in gliomas. Cancer Treat Res. 2004; 117:249–62. [PubMed: 15015564]
36. Cinatl J, Speidel D, Hardcastle I, Michaelis M. Resistance acquisition to MDM2 inhibitors. Biochem Soc Trans. 2014; 42(4):752–7. [PubMed: 25109953]
37. Costa B, Bendinelli S, Gabelloni P, Da Pozzo E, Daniele S, Scatena F, et al. Human glioblastoma multiforme: p53 reactivation by a novel MDM2 inhibitor. PLoS One. 2013; 8(8):e72281. [PubMed: 23977270]
38. Phelps D, Bondra K, Seum S, Chronowski C, Leasure J, Kurmasheva RT, et al. Inhibition of MDM2 by RG7388 confers hypersensitivity to X-radiation in xenograft models of childhood sarcoma. Pediatr Blood Cancer. 2015; 62(8):1345–52. [PubMed: 25832557]
39. Werner LR, Huang S, Francis DM, Armstrong EA, Ma F, Li C, et al. Small molecule inhibition of MDM2-p53 interaction augments radiation response in human tumors. Mol Cancer Ther. 2015
40. Zhang Z, Ding Q, Liu JJ, Zhang J, Jiang N, Chu XJ, et al. Discovery of potent and selective spiroindolinone MDM2 inhibitor, RO8994, for cancer therapy. Bioorg Med Chem. 2014; 22(15): 4001–9. [PubMed: 24997575]
41. Ding Q, Zhang Z, Liu JJ, Jiang N, Zhang J, Ross TM, et al. Discovery of RG7388, a potent and selective p53-MDM2 inhibitor in clinical development. J Med Chem. 2013; 56(14):5979–83. [PubMed: 23808545]
42. Ohnstad HO, Castro R, Sun J, Heintz KM, Vassilev LT, Bjerkehagen B, et al. Correlation of TP53 and MDM2 genotypes with response to therapy in sarcoma. Cancer. 2013; 119(5):1013–22. [PubMed: 23165797]
43. Pishas KI, Neuhaus SJ, Clayer MT, Schreiber AW, Lawrence DM, Perugini M, et al. Nutlin-3a efficacy in sarcoma predicted by transcriptomic and epigenetic profiling. Cancer Res. 2014; 74(3): 921–31. [PubMed: 24336067]
44. Weller M, Felsberg J, Hartmann C, Berger H, Steinbach JP, Schramm J, et al. Molecular predictors of progression-free and overall survival in patients with newly diagnosed glioblastoma: a prospective translational study of the German Glioma Network. J Clin Oncol. 2009; 27(34):5743–50. [PubMed: 19805672]

Significance Statement

Glioblastoma (GBM) is the most aggressive brain cancer. Despite intensive treatments, the prognosis of GBM patients remains poor. Thus, new therapies are urgently needed to improve patients' outcome. Research efforts worldwide have identified key molecular abnormalities involved in GBM growth, including p53 pathway disruption via *MDM2 or MDM4* gene amplification, collectively observed in 15–18% of GBM cases. Here, we show that treatment of *MDM2*-amplified and other TP53 wild-type patient-derived GBM models with RG7112, an MDM2 inhibitor, induces tumor cell death, reduces tumor growth and increases survival. These data strongly support evaluation of MDM2 inhibitors in clinical trials enrolling *MDM2*-amplified as well as a subset of *TP53* wild-type GBM patients that remains to be defined.

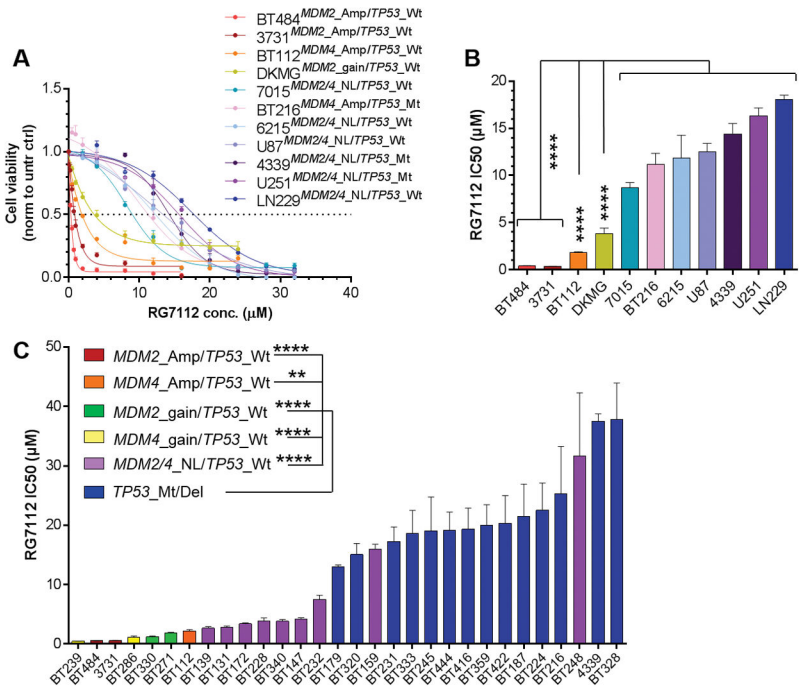

Figure 1.

Effects of RG7112 on cell proliferation and viability of GBM lines with various alterations of p53 pathway **A)** Cohort #1 (Amp: amplification, Mt: homozygous mutation, Wt: wild-type, NL: normal level): Proliferation and viability was 72 h after exposure to various concentrations of RG7112 on GBM cells carrying normal levels of *MDM2* or *MDM4* gene, and/or TP53 mutation (cold colors), or amplification of *MDM2* or *MDM4* gene, and a wild-type form of TP53 (warm colors). In this series, all lines with *MDM2/4* amplification have Wt *TP53*, and all *TP53* mutated lines have normal levels of *MDM2/4* genes. **B)** Cohort #1: RG7112 IC50s (concentrations for which a 50% decrease in cell viability and proliferation was observed) in each cell line tested. **C)** Cohort #2: RG7112 IC50s in *MDM2/4* amplified/gained cell lines, *TP53* mutated/deleted cell lines, or cell lines with none of these alterations (*MDM2/4*_NL/*TP53*_Wt lines).

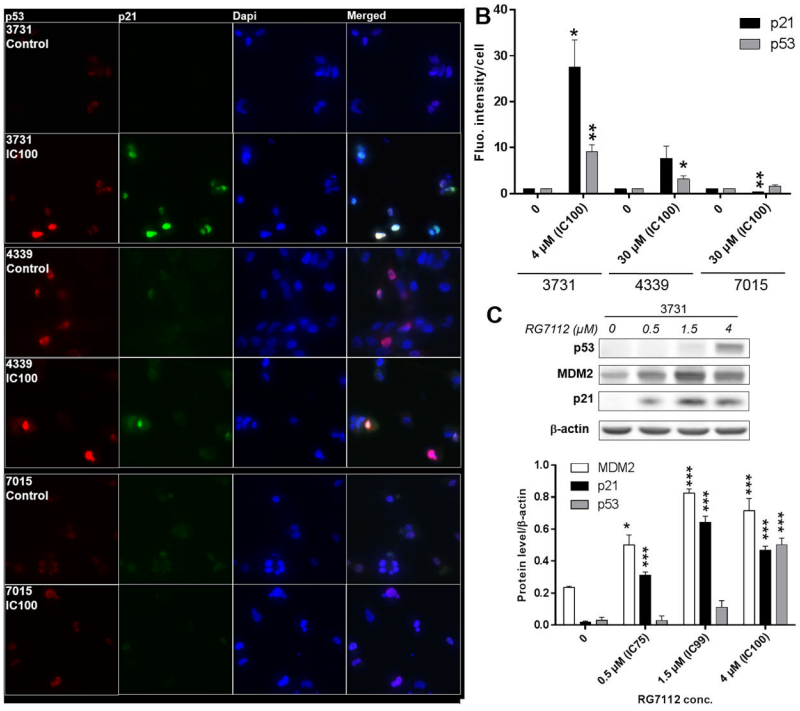

Figure 2.

p53 and p21 protein levels in GBM lines with or without *MDM2* gene amplification and treated with RG7112. **A)** Representative immunofluorescence images of 3731*MDM2*_Amp/*TP53*_Wt, 4339*MDM2/4*_NL/*TP53*_Mut, and 7015*MDM2/4*_NL/*TP53*_Wt treated or not with RG7112. p53 (red), p21 (green) and cell nuclei (blue) can be seen. **B)** Protein levels were quantified by three independent immunofluorescence assays. Each bar represents the fluorescence intensity per cell normalized over the value obtained in the corresponding untreated control cells. **C)** p53, p21 and MDM2 protein levels in MDM2-amplified GBM line treated with RG7112.

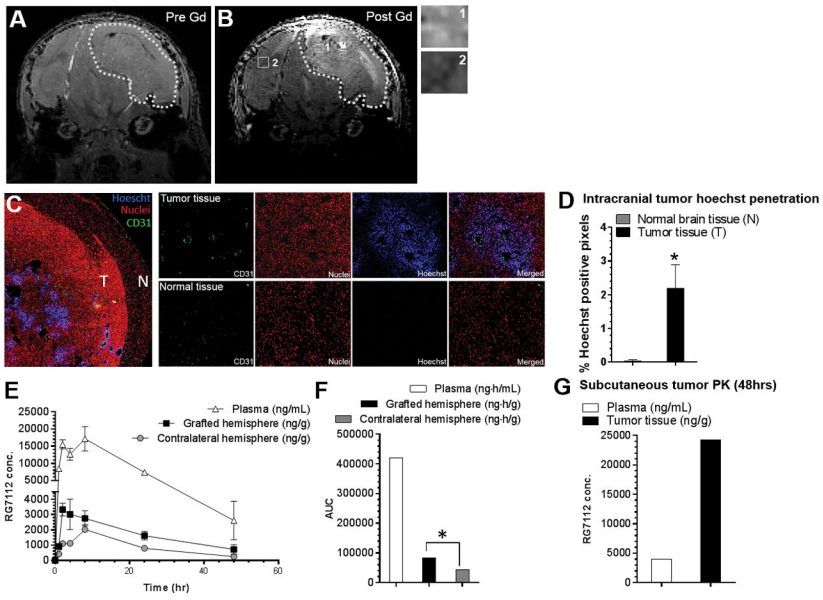

Figure 3.

Assessment of the permeability of the blood-brain barrier in the *MDM2*-amplified orthotopic model and its impact on RG7112 pharmacokinetic distribution. MRI imaging of 3731*MDM2*_Amp/*TP53*_Wt xenograft. T1-weighted image A) before and B) after gadolinium injection are shown, with close-ups of tumor (1) and normal (2) tissue. Dotted line shows the outline of the tumor. **B)** Penetration of Hoechst 33342 in normal (N) and tumor tissue (T) after Hoechst intravenous injection. CD31 (green), nuclei (propidium iodide: red), Hoechst (blue) and a merged image can be seen. **C)** Hoechst staining was quantified in the tumor tissue compared to the normal brain tissue. **D)** Pharmacokinetic distribution of RG7112 in brain tissue of grafted and contralateral hemisphere and plasma after administration of a 100 mg/kg single dose. RG7112 was quantified by mass spectroscopy. E) Area-under-the-curves (AUCs) calculated from the pharmacokinetic data over a 48 hrs period. F) Drug distribution in subcutaneous tumor and plasma 48 h after RG7112 administration. *p-value < 0.05 between grafted hemisphere or tumor tissue compared to contralateral hemisphere or normal brain tissue.

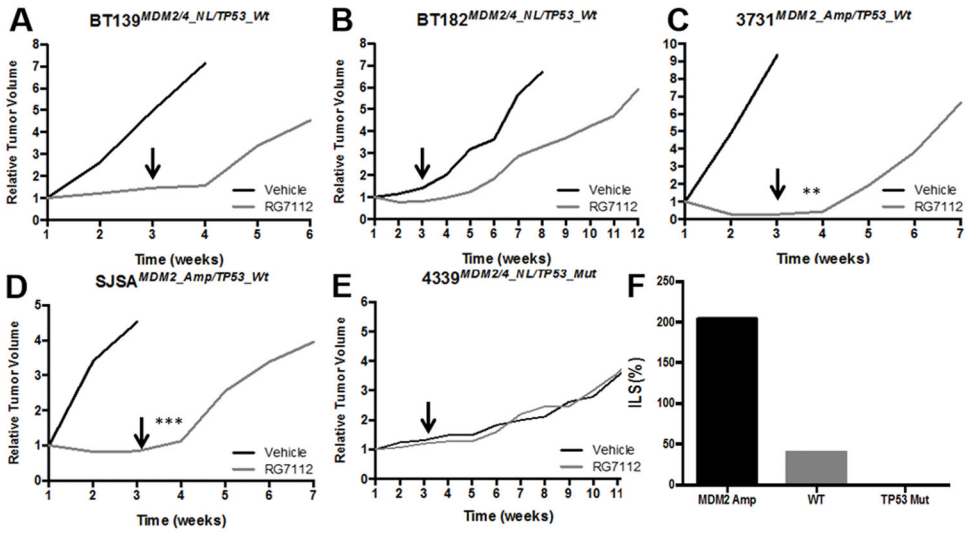

Figure 4.

Effect of RG7112 in GBM patient subcutaneous xenografts on tumor growth overtime of GBM lines with various alterations. **A–B)** *MDM2/4* and *TP53* wild-type cell line, **C)** *MDM2* amplification and *TP53* wild-type cell line and **D)** *MDM2/4* normal level and *TP53* mutant cell line. **E)** *MDM2*-amplified osteosarcoma model was included as a positive control. Once tumor was established, animals were treated with RG7112 or vehicle formulation for 3 weeks. Arrows show the end of treatment period. **F)** Effect of RG7112 on increased life span in *MDM2*-amplified tumor (3731), *TP53* wild-type tumors (BT139 and BT182), and *TP53* mutant tumor (4339).

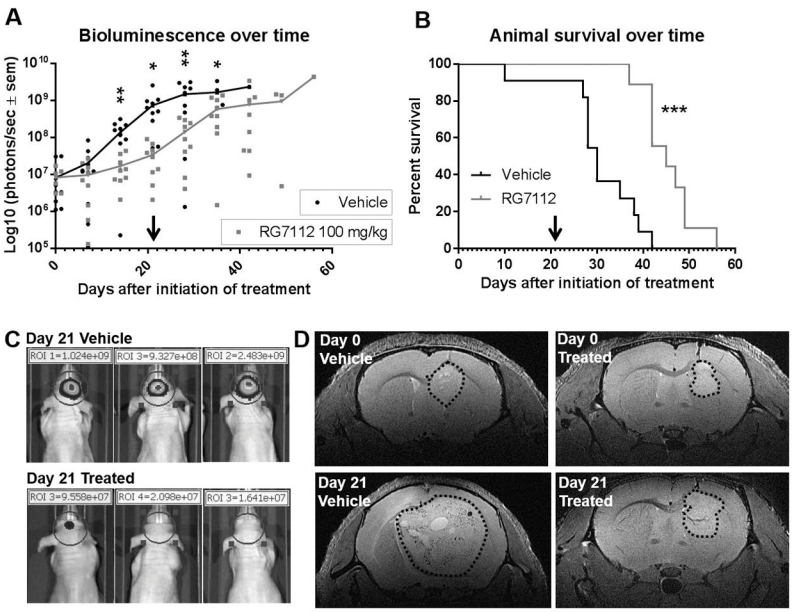

Figure 5.

Effect of RG7112 in 3731*MDM2*_Amp/*TP53*_Wt GBM orthotopic xenograft. **A)** Bioluminescence signal measured overtime. Each dot represents value for one animal. **B)** Animal survival. Once tumor was established, animals were treated with RG7112 or vehicle formulation for 3 weeks. Bioluminescence signal was measured weekly. Arrow shows the end of treatment period. **C)** Three representative animals from each group are shown after the end of treatment period (21 days) with bioluminescence signal acquired with a 0.5 second exposure time. **D)** MRI imaging (T2-weighted) of a vehicle and RG7112-treated animal prior to and at the end of the treatment period. Dotted line shows the outline of tumors.

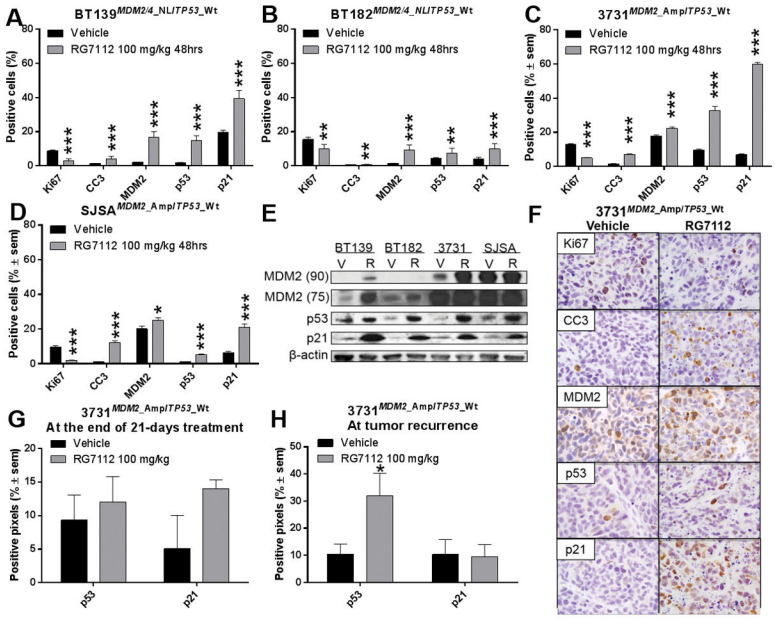

Figure 6.

Quantification of markers of response to RG7112. **A–D)** Quantification of Ki67, CC3, MDM2, p53 and p21 protein level by immunohistochemistry of: **A–B**) *MDM2/4* and *TP53* wild-type cell line, **C**) *MDM2* amplification and *TP53* wild-type cell line and **D**) *MDM2*-amplified osteosarcoma positive control, harvested 48 h after one dose of RG7112. **E**) Western immunoblot analysis of subcutaneous tumors showing MDM2 75 and 90 kDa forms, p53 and p21 proteins. **F**) Representative images showing marker staining in brown and nuclei in blue of vehicle and RG7112 treated 3731*MDM2*_Amp/*TP53*_Wt tumor. **G**) Quantification of p53 and p21 protein levels on the day after the 21 day treatment period, or **H**) at the moment of termination when animals showed signs of tumor-associated illness due to relapse after treatment.